

# Breakup Characteristics of Laminar and Turbulent Liquid Sheets Formed by Impinging Jets in High Pressure Environments

K. Jung, T. Khil, B. Lim and Y. Yoon

School of Mechanical and Aerospace Engineering, Seoul National University  
San 56-1 Shinlim-dong Kwanak-ku, Seoul 151-742  
jkihoon@snu.ac.kr

Keywords: liquid sheet breakup, impinging jet, high pressure spray

## Abstract

Breakup characteristics of liquid sheets formed by the impingement of two water jets, such as a breakup length and a breakup wavelength of sheet, were investigated as increasing the injection velocity up to 30m/s and the ambient gas pressure up to 4.0MPa. While round edged orifices formed a laminar sheet which has no waves on the sheet when the injection velocity is low, sharp edged orifices formed a turbulent sheet which has impact waves irrespective of the injection velocity. Thus we compared the differences of breakup characteristics between them. The results showed that the aerodynamic force significantly affects the breakup of laminar sheet when the gas based Weber number is higher than unity. It was also found that the turbulent sheets have three breakup regimes, i.e. expansion regime, wave breakup regime and catastrophic breakup regime according to the gas based Weber number.

## Introduction

Impinging type injectors that atomize liquid mass into fine drops using the impinging momentum of liquid jets are commonly used in liquid rocket engines due to their advantages: low manufacturing cost, potentially high flow rate, compatibility of chamber wall and so forth<sup>1)</sup>. Hence, extensive experimental and analytical researches have been carried out on the spray characteristics of the injector, especially, the breakup of liquid sheets formed by the impingement of two liquid jets<sup>2-6)</sup>.

Dombrowski and Hooper found that the flow characteristics of liquid jets, which is dominated by the shape of orifice entrance and the jet velocity, strongly affects both the formation and breakup of liquid sheet<sup>2)</sup>. When two liquid jets impinge and form a sheet, impact waves are formed on the sheet. If the jets are laminar flows which have boundary layers, the impact waves are damped. If the jets are turbulent flows, however, the impact waves are not damped and strongly affects the sheet breakup because they do not have the damping boundary layers. Thus, the laminar sheet formed by the laminar jets (Fig. 1(a)) is wider and steadier than the turbulent sheet formed by the turbulent jets (Fig. 1(b)). The laminar sheets are disintegrated by the waves formed by the aerodynamic force of ambient gas, and thus the linear instability theory, which is based on the balance between the aerodynamic force of ambient gas and the surface

tension of liquid sheet, has been successfully applied to modeling the spray characteristics: e.g. sheet breakup length, breakup wavelength, drop size and so forth<sup>3-4)</sup>. However, analytic solutions for the turbulent sheets have shown disagreements with experimental results<sup>5)</sup> because the effects of the impact force on the formation and development of the waves which induce the sheet breakup has not been clearly understood. Recently, Strakey and Talley reported that the impact force and the aerodynamic force determine the sheet breakup in the case of low ambient gas pressure and high, respectively, but they did not suggest a quantitative result for the sheet breakup<sup>6)</sup>.

In present study, we focused on the effects of ambient gas density on the breakup characteristics of both the laminar and turbulent sheets. Also, we suggested empirical relations on the sheet breakup characteristics: the sheet breakup length defined as the distance from the impingement point to the edge of liquid sheet along the x-axis ( $x_b$  in Fig. 1) and the sheet breakup wavelength defined as the wavelength on the sheet at the moment of the sheet breakup ( $\lambda_b$  in Fig. 1).

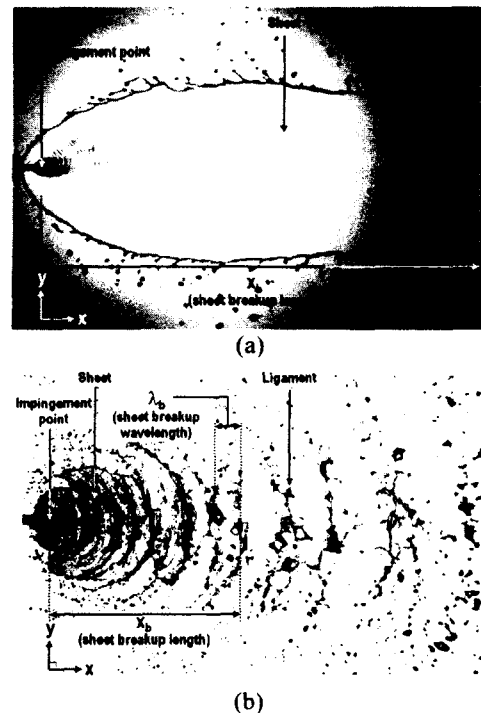


Fig. 1 Spray pattern of like-doublet: (a) laminar and (b) turbulent sheet.

## Experimental Method

### Injector Design

In order to obtain the laminar and the turbulent sheet, we designed round and sharp edged orifices as shown in Fig. 2. Since Vennard showed that the orifice of which entrance is rounded with 0.14 times of orifice diameter or much has no a vena contracta<sup>7)</sup>, the round edged orifice was designed with a curvature radius of one diameter of orifice. Both the orifice diameters were 0.07cm and the ratios of orifice length to diameter were designed as 20, which is higher than those of practical impinging type injectors, in order to induce more steady flow. The impingement point of two liquid jets was fixed at the location of five times of orifice diameter from the orifice exit and the impingement angle of two liquid jets was designed as 60 degrees angle. The steel mesh and the sub-chamber were designed to uniformly supply water used as fuel stimulant to the orifices by suppressing a flow recirculation at upstream of injector chamber.

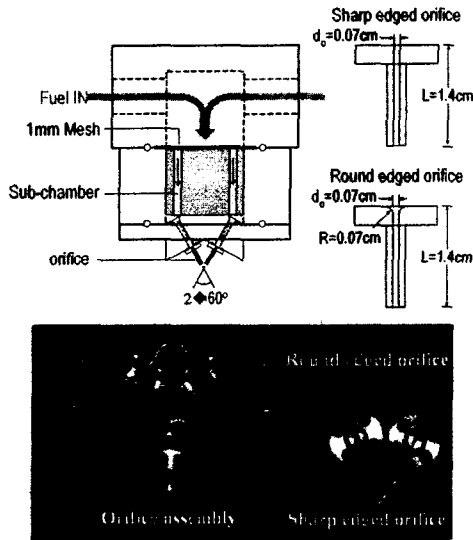


Fig. 2 Schematic and photography of impinging jet injector using round and sharp edged orifices.

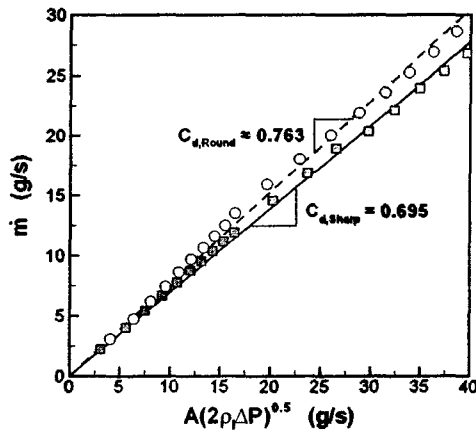


Fig. 3 Discharge coefficients of round and sharp edged orifices.

Figure 3 shows the discharge coefficients of the round and sharp edged orifices. As expected, the discharge coefficient of round edged orifice was higher than that of sharp edged orifice. It is general that the cavitation bubbles occur inside the sharp edged orifice, which reduces the discharge coefficient, but the decrease was not found inside the present orifices. The reason is thought that the connecting orifice between sub-chamber and orifice interrupted the formation of vena contracta at the entrance of orifice. Thus, we did not consider the cavitation which affects the spray characteristics<sup>8,9)</sup>.

### High Ambient Pressure System

Our high ambient pressure system includes four parts: main chamber, liquid fuel supply tanks, gas supply tanks and controller. The nitrogen gas is pressurized into the main chamber up to 6MPa and the fuel simulant is supplied into the chamber with the pressure added by the chamber pressure and injection pressure difference, which are set by controller. Since the pressure of chamber builds up when the spray is injected, the increment must be exhausted, and the controller automatically determines this by sensing the chamber pressure and opening and closing the exhaust valve. In addition, the injection pressure slowly decreases because the gas volume increases in the fuel supply tanks as the liquid simulant is injected, and thus the controller supplements the pressure in the similar method. The gas-curtain systems are set in four windows in order to reduce the deposition of droplets on the inner window surfaces. The pressure increment by the injection of gas-curtain is also exhausted by the controller.

The main chamber of Fig. 4 was designed for operating up to 6MPa; the endurance pressure was designed as 12MPa for safety. The diameter and volume of chamber is 500mm and 200l, respectively. This volume was considered for operating during 5 minutes for the maximum flow rate of present injectors. Transporting device of injector on the chamber cover was designed to operate under pressurized conditions.

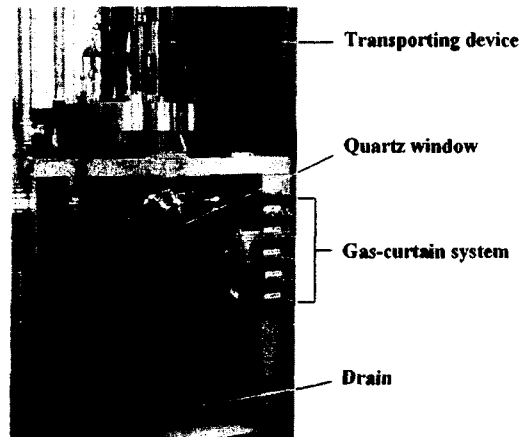


Fig. 4 High pressure chamber

### Sheet Shape Changes

Figure 5 shows the effects of ambient gas pressure  $P_c$  and injection velocity  $U_j$  on the shapes of laminar sheets. First of all, it was found that the laminar sheet which damps the impact waves is not shown above the injection velocity of  $15m/s$ . The reason is thought that the impact force is too strong for the jet boundary layer of low velocity to damp after the velocity. Therefore, we focused on only the laminar sheets are formed when the injection velocity is lower than  $15m/s$ .

The laminar sheet shapes were compared with analytic solutions which is based on the mass and the momentum conservations<sup>10)</sup>; contrary to the present experimental results, the solutions are independent on the ambient pressure so that the shapes were compared only at  $0.1MPa$ . It was found that the solutions underestimate the size of sheet at the low injection velocity of  $3m/s$  and overestimate it at the high injection velocity of  $7m/s$  or  $10m/s$ . In other words, the analytic solutions overestimate the effects of injection velocity on the sheet shape. Also, the analytic solution expect that the breakup length of sheet is proportional to the square of injection velocity<sup>4)</sup>, but the experimental results show that it is not so sensitive to the injection velocity.

According to the linear instability theory<sup>5)</sup>, the disturbances on the sheet are amplified by the aerodynamic force of ambient gas and their growths induce the sheet breakup, and thus the breakup length

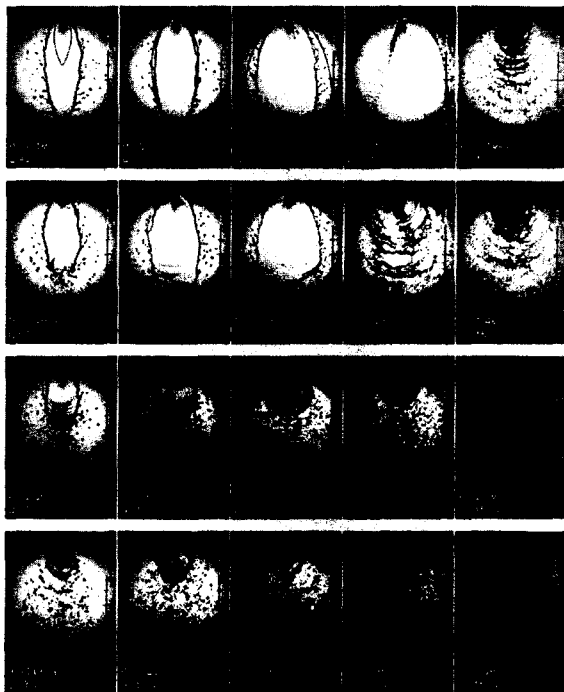


Fig. 5 Changes of laminar sheet shapes as functions of injection velocity and ambient pressure (solid lines at  $P_c=0.1MPa$  show sheet shapes obtained from Ibrahim and Przekwas's results<sup>10)</sup>).

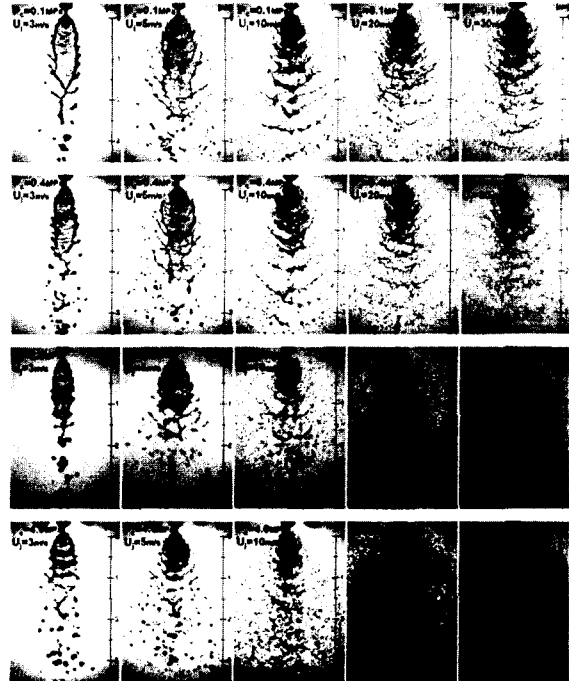


Fig. 6 Changes of turbulent sheet shapes as functions of injection velocity and ambient pressure.

decreases as the ambient gas density increases. This can be confirmed by Fig. 5 which shows the waves appear on the sheet after the high ambient pressure of  $2.0MPa$ .

As for the turbulent sheets, the waves exist on the sheet in all experimental conditions because the impact waves are not damped as shown in Fig. 6. The waves formed primarily by the impact force can be easily amplified by the aerodynamic force, and thus it is expected that the breakup length of turbulent sheet is shorter than that of laminar sheet under the same condition.

From Figs. 5 and 6, it was found that the shape of laminar sheet is definitely different with that of turbulent sheet due to the damping effects of laminar sheet in the cases that both the injection velocity and ambient pressure are low. As the injection velocity increases, however, the boundary layer can damp the impact waves no more, and thus both shapes become similar (e.g.  $15m/s$  velocity cases under  $0.1MPa$  pressure). In addition, since the growth rates of waves inside the sheets become very high at the high ambient pressure, the difference between the laminar and the turbulent sheet disappears (e.g.  $3.0MPa$  pressure cases at  $7m/s$  velocity). It is thought, therefore, that the differences of the spray patterns due to the shape of orifice entrance are not significant in practical combustion chambers where the injection velocity and the ambient pressure are very high.

### Breakup Length and Breakup Wavelength

#### Laminar Sheet Breakup

As shown in Fig. 5, the waves which break the sheet

did not exist below 0.4MPa, and thus we focused on only the breakup length of sheet. In order to consider both the injection velocity and ambient gas pressure (or density) with one parameter, a gas based Weber number  $We_g$  was defined as following:

$$We_g = \frac{\rho_g U_j^2 d_o}{\sigma} \quad (1)$$

where  $\rho_g$  indicates the density of ambient gas. According to the definition,  $We_g$  means the ratio of aerodynamic force to surface tension force, and  $We_g$  increases as the injection velocity or the ambient gas pressure increases.

Figure 7 shows the breakup lengths as a function of  $We_g$ . One hundred images were measured for one experimental case, and the deviations of data were less than 10 percents of their mean values. The most interesting finding is that the breakup length shows different tendency before and after  $We_g$  is about unity. In the cases that  $We_g$  is lower than unity, the aerodynamic force which induces the sheet breakup is so weak that the sheet is expanded by the increment of mass flow rate as increasing the jet Weber number  $We_j$  as shown in Fig. 7(a). However, the breakup length

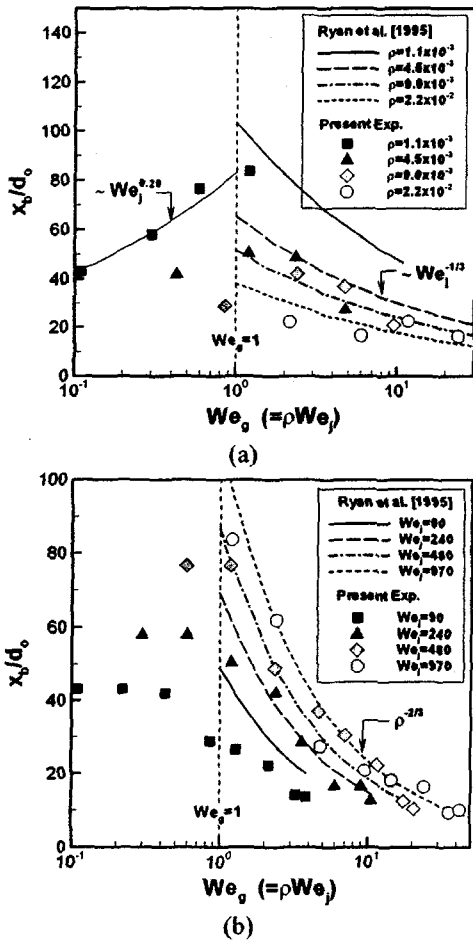


Fig. 7 Breakup lengths of laminar sheets as a function of  $We_g$ : as increasing (a) jet Weber number  $We_j$  and (b) density ratio of gas to liquid  $\rho$ .

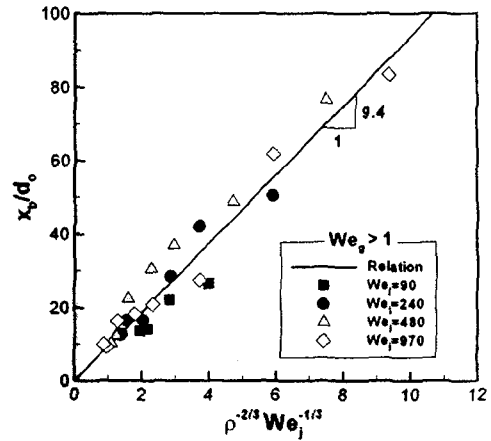


Fig. 8 Empirical relation for breakup lengths of laminar sheets when  $We_g$  is higher than unity.

was not proportional to  $We_j$  like Ibrahim and Przekwas's model<sup>10)</sup> but to  $We_j^{0.29}$ . From the difference, it can be expected that the thickness at the sheet edge is thicker than expected thickness. Also, Fig. 7(b) shows the breakup lengths are not significantly changed as increasing the ambient gas density when  $We_g$  is lower than unity. Therefore, it is thought that the aerodynamic force does not significantly affect the laminar sheet breakup and the sheets are expanded by the increase of mass flow rate until  $We_g$  is lower than unity.

In the cases that  $We_g$  is higher than unity, however, the sheets are broken by the aerodynamic force. Since the laminar sheet damps the effect of impact force on the sheet breakup, the sheet breakup are dominated by only the aerodynamic force, and thus the breakup lengths agree well with the linear instability theory of Ryan et al.<sup>5)</sup> as shown in Figs. 7(a) and (b). Therefore, the breakup of laminar sheet can be expected by the theory only if  $We_g$  is higher than unity. Figure 8 shows the comparison between the experimental results and the following empirical relation when  $We_g$  is higher than unity:

$$\frac{x_b}{d_o} = 9.4 \rho^{-2/3} We_j^{-1/3} \quad (We_g > 1). \quad (2)$$

The indexes of parameters of above equation are same with Ryan et al.'s<sup>5)</sup> and Huang's results<sup>11)</sup>, but the constant 9.4 is in between Ryan et al.'s 10.41 and Huang's 7.1.

#### Turbulent Sheet Breakup

As shown in Fig. 6, the turbulent sheets have the waves formed by the impact of two jets irrespective of  $We_g$ . In fact, however, the waves do not contribute the sheet breakup at the low  $We_g$ , e.g. when  $U_j=3$  or  $5m/s$  at  $P_c=0.1MPa$ . In these cases, the periodicity of drop formation is not shown, and thus we considered that the cases do not have the breakup wavelengths. Also, the breakup length as well as the breakup wavelength could not be defined in the cases of very high  $We_g$ , e.g. when  $P_c=2.0$  or  $4.0MPa$  at  $U_j=30m/s$ . Figure 9 shows

these limits for the breakup length and the breakup wavelength. The symbols  $\blacktriangle$  and  $\nabla$  were marked when the breakup length and breakup wavelength exist at the given condition, respectively.

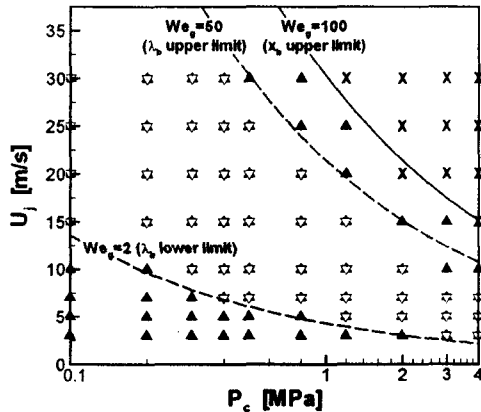


Fig. 9 Breakup criteria of turbulent sheet ( $\blacktriangle$  and  $\nabla$  were marked when the breakup length  $x_b$  and breakup wavelength  $\lambda_b$  exist at the given condition, and X were marked when both do not exist).

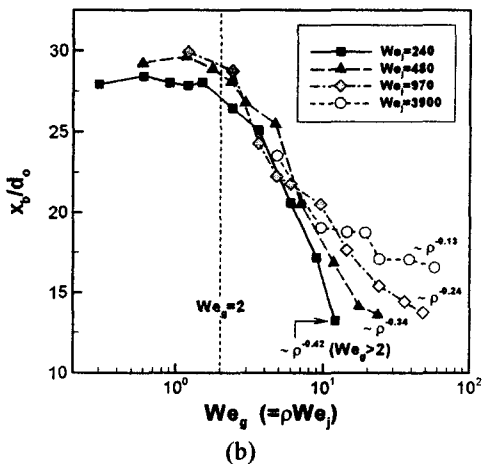
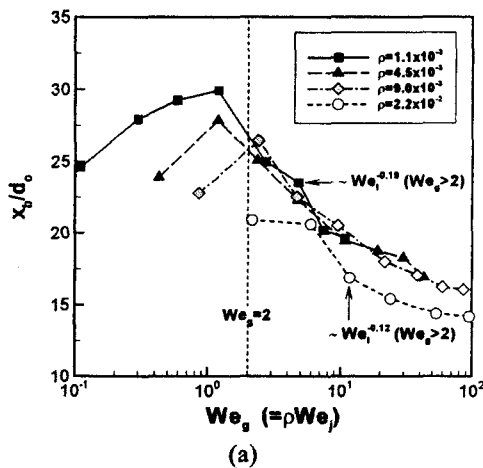


Fig. 10 Breakup lengths of turbulent sheets as a function of  $We_g$ : as increasing (a) jet Weber number  $We_j$  and (b) density ratio of gas to liquid  $\rho$ .

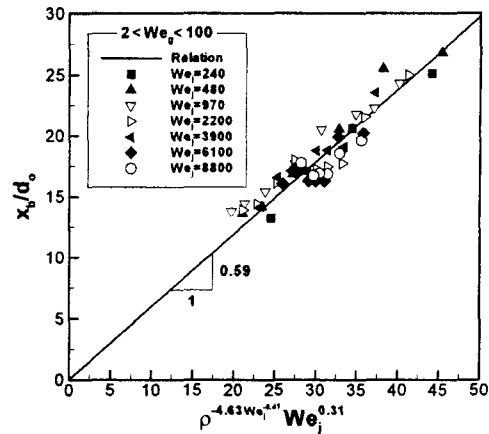


Fig. 11 Empirical relation for breakup lengths of turbulent sheets when  $2 < We_g < 100$ .

From Fig. 9, it was found that the turbulent sheet has three breakup regimes. First, the sheet breakup is not controlled by waves so that the breakup periodicity does not appear and the breakup length increases as increasing jet velocity when  $We_g$  is lower than about 2. While this sheet expansion regime is also found in the laminar sheet breakup, the criterion of turbulent sheet ( $We_g=2$ ) is higher than that of laminar sheet ( $We_g=1$ ). The reason is thought that the sheet thickness of turbulent sheet is thicker because its area is more narrow so that the growth rate of waves on the turbulent sheet is lower than that of laminar sheet, and thus the aerodynamic force can affect the sheet breakup at the higher  $We_g$ . As  $We_g$  increases, the wave breakup regime where the turbulent sheet breakup is determined by the growth of waves appears until  $We_g$  is lower than 100. Since the sheets are broken by waves, the breakup periodicity appears. Although it was impossible to properly measure the breakup wavelength when  $We_g$  is higher than 50 because the spray is too dense, it is obvious that the sheets are broken by the waves. However, the sheets are broken just after injection by the strong aerodynamic force when  $We_g$  is higher than 100 so that the breakup length as well as the breakup wavelength could not be discriminated in this catastrophic breakup regime.

Figure 10 shows the breakup lengths of turbulent sheets as a function of  $We_g$ . As shown in Fig. 11(a), the breakup lengths increase as increasing the jet Weber number  $We_j$  at the sheet expansion regime where  $We_g$  is lower than 2. In this regime, the aerodynamic force does not affect the turbulent sheet breakup as shown in Fig. 10(b). Further increase of  $We_g$ , the impact waves are grown by the aerodynamic force so that the breakup length decreases. The linear instability theory expects that the breakup length is proportional to  $\rho^{-0.67}$ . However, the effect of ambient gas density becomes mitigated as the jet Weber number increases; from  $\rho^{-0.42}$  at  $We_j=240$  to  $\rho^{-0.13}$  at  $We_j=3900$ . This can be explained by the effect of the impact force. As the injection velocity increases, the

impact force becomes so strong that the amplitudes of waves are high enough to break the sheet without the amplification by the aerodynamic force. Therefore, the effect of ambient gas pressure is dependent on the injection velocity, i.e. jet Weber number. From the results, a following empirical relation on the breakup length of turbulent sheet could be obtained:

$$\frac{x_b}{d_o} = 0.59 \rho^{-4.63 We_j^{-0.41}} We_j^{0.31} \quad (2 < We_g < 100) \quad (3)$$

where  $We_j^{0.31}$  was used compensate the effect of  $We_j$  in  $\rho^{-4.63 We_j^{-0.41}}$ , and thus it has not a physical meaning.

Figure 12 shows the breakup wavelengths of turbulent sheets as functions of the jet Weber number  $We_j$  and the density ratio of gas to liquid  $\rho$ . From Fig. 12(a), it was found that the wavelength is proportional to  $We_j^{-0.18}$  until  $\rho=0.0090$ . Under the higher ambient density, the wavelengths become more sensitive to the jet Weber number up to  $We_j^{-0.37}$  when  $\rho=0.045$ , which results from the increase of the aerodynamic force. According to the linear instability theory<sup>3,5)</sup>, however, the wavelength is proportional to  $We_j^{-1}$ , thus it is thought that the theory overestimates the effect of injection velocity.

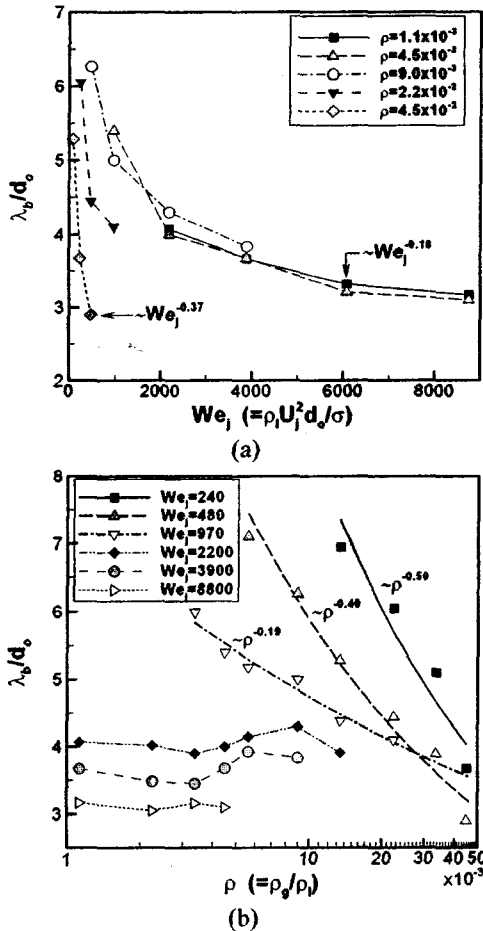


Fig. 12 Breakup wavelengths of turbulent sheets as functions of (a) jet Weber number  $We_j$  and (b) density ratio of gas to liquid  $\rho$ .

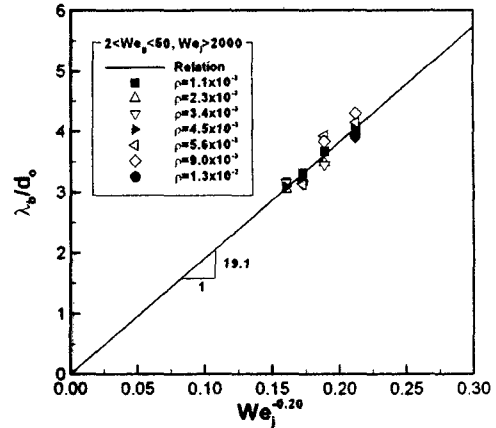


Fig. 13 Empirical relation for breakup wavelengths of turbulent sheets when  $We_g$  is higher than 2 and lower than 50 and  $We_l$  is higher than 2000.

The overestimation is also shown in the effect of ambient gas pressure; although the theory expects that the breakup wavelength is proportional to  $\rho^{-1}$ , the experimental results of Fig. 12(b) were less sensitive to the ambient gas density. It is interesting that the wavelengths are not affected by the ambient gas pressure after the jet Weber number is higher than 2000. This means the aerodynamic force is not significant for the sheet breakup wavelength only if the injection velocity is high enough. This result is contrary to the present results of laminar sheet and Strakey and Talley's results of turbulent sheet<sup>6)</sup>. It is thought that the impact force is strong enough to entirely break the sheet before the waves from the impact force are amplified by the aerodynamic force, and thus the effects of aerodynamic force is not significant in those cases. It is obvious, of course, that the aerodynamic force significantly affects the following breakup processes such as the breakup of ligaments into drops or the secondary breakup of drops.

Since the jet Weber number may be higher than 2000 in practical cases, we considered an empirical relation in the cases  $We_j$  is higher than 2000:

$$\frac{\lambda_b}{d_o} = 19.1 We_j^{-0.20} \quad (2 < We_g < 50, We_j > 2000) \quad (4)$$

Figure 13 shows the comparison between the experimental results and the above empirical relation.

#### Nomenclature

$A$	orifice cross sectional area
$C_d$	orifice discharge coefficient
$d_o$	orifice diameter
$L$	orifice length
$\dot{m}$	spray mass flow rate
$P_c$	ambient gas pressure
$R$	entrance curvature radius of round edged orifice
$U_j$	jet injection velocity
$We_j$	jet Weber number, $\rho_l U_j^2 d_o / \sigma$

$We_g$	jet Weber number based on gas density, $\rho_g U_j^2 d_o / \sigma$
$x_b$	sheet breakup length, i.e. distance from impingement point to sheet edge
$\Delta P$	injection pressure difference
$\lambda_b$	sheet breakup wavelength, i.e. distance from last wave on sheet to sheet edge
$\theta$	half impingement angle of liquid jets
$\rho$	ratio of ambient gas density to liquid density
$\rho_l$	liquid density
$\rho_g$	ambient gas density
$\sigma$	surface tension

### Conclusion

The results of the measurements of spray characteristics under the high ambient pressure showed that the aerodynamic force significantly affects the breakup of laminar sheet when the aerodynamic force is higher than the surface tension force, i.e.  $We_g$  is higher than unity. When  $We_g$  is lower than unity, however, the laminar sheet expands as increasing the injection velocity and the aerodynamic force does not affect the sheet breakup.

The breakup characteristics of turbulent sheets had three regimes, i.e. expansion regime, wave breakup regime and catastrophic breakup regime according to  $We_g$ . Under the expansion regime, the sheet breakup length increases as increasing injection velocity and the aerodynamic force does not affect the breakup length. Under the wave breakup length regime, the breakup length decreases as the injection velocity and the ambient gas density increase due to the aerodynamic force. However, the effect of aerodynamic force becomes mitigated as increasing jet Weber number. In this regime, the breakup wavelength decreases as increasing the injection velocity or the ambient gas density, but the ambient gas density does not affect the wavelength only if the jet Weber number is higher than 2000. Under the catastrophic breakup regime, the breakup length as well as the breakup wavelength could not be discriminated.

### Acknowledgments

This research was supported by National Research Laboratory program (M1-0104-00-0058). The authors wish to acknowledge this financial support.

### References

- 1) Gill, G. S. and Nurick, W. H.: Liquid Rocket Engine Injectors, *NASA SP-8089*, 1976.
- 2) Dombrowski, N. and Hooper, P. C.: A Study of the Sprays Formed by Impinging Jets in Laminar and Turbulent Flow, *Journal of Fluid Mechanics*, **18** (3), 1964, pp. 392-400.
- 3) Squire, H. B.: Investigation of the Instability of a Moving Liquid Film, *British Journal of Applied Physics*, **4**, 1953, pp. 167-169.
- 4) Dombrowski, N. and Hooper, P. C.: The Effect of Ambient Density on Drop Formation in Sprays, *Chemical Engineering Science*, **17**, 1962, pp. 291-305.
- 5) Ryan, H. M., Anderson, W. E., Pal, S. and Santoro, R. J.: Atomization Characteristics of Impinging Liquid Jets," *Journal of Propulsion and Power*, **11** (1), 1995, pp. 135-145.
- 6) Strakey, P. A. and Talley, D. G.: Spray Characteristics of Impinging Jet Injectors at High Back-Pressure, *8<sup>th</sup> ICLASS*, July 2000.
- 7) Vennard, J. K.: *Elementary Fluid Mechanics*, Wiley, New York, 1961.
- 8) Nurick, W. H.: Orifice Cavitation and Its Effect on Spray Mixing, *Journal of Fluids Engineering*, Dec., 1976, pp. 681-687.
- 9) Tamaki, N., Shimizu, M., Nishida, K. and Hiroyasu, H.: Effects of Cavitation and Internal Flow on Atomization of a Liquid Jet, *Atomization and Spray*, **8**, 1998, pp. 179-197.
- 10) Ibrahim, E. A. and Przekwas, A. J.: Impinging Jets Atomization, *Physics of Fluids A*, **3**, 1991, pp. 2981-2987.
- 11) Huang, J. C. P.: The Break-Up of Axisymmetric Liquid Sheets, *Journal of Fluid Mechanics*, **43** (2), 1970, pp. 305-319.